

Ab-initio description of hole localization and Zhang-Rice singlets in one-dimensional doped cuprates

Alessio Filippetti and Vincenzo Fiorentini

CNR-INFM SLACS and Department of Physics, University of Cagliari, I-09042 Monserrato (CA), Italy

(Dated:)

We present the first ab-initio band-theory-based description of spin-compensated polarons (known as Zhang-Rice singlets) in a hole-doped cuprate, specifically one-dimensional $\text{Ca}_{2+x}\text{Y}_{2-x}\text{Cu}_5\text{O}_{10}$. Zhang-Rice singlets are many-particle configurations relevant to the exotic behavior of hole-doped cuprates, stemming from spontaneous charge localization. They appear in our case-study material above a threshold doping, successively turning the insulating undoped antiferromagnet into a gap insulator, a singlet-rich metallic paramagnet, and finally, a singlet-saturated insulating diamagnet.

PACS numbers:

An outstanding challenge in condensed matter theory is the thorough understanding of the electronic structure of hole-doped cuprates. A key ingredient of the physical properties of many such materials is thought to be a multiparticle electronic state known as spin-compensated polaron or Zhang-Rice singlet (ZRS in the following), first introduced by Zhang and Rice [1] in the context of underdoped cuprate superconductors. A ZRS is in essence a localized, positively-charged spin-singlet state appearing when (a fractions of) a doping hole localizes on one or more O's first-neighbor of the Cu^{2+} site of a CuO_2 unit (embedded in e.g. a stripe or layer), coupled antiferromagnetically to the polarized native Cu hole.

There is ample evidence of the presence of ZRS in doped cuprates. Beside their observation [2] in superconductors and their relevant role therein [3], experiments [4, 5, 6, 7] indicate that the prototypical one-dimensional (1D) cuprate $\text{Ca}_{2+x}\text{Y}_{2-x}\text{Cu}_5\text{O}_{10}$ (henceforth CaYCuO) must be highly populated by ZRS in a specific doping range. In this paper we study CaYCuO by a fully first-principles band theory (the pseudo-self-interaction correction approach [8], already applied to other correlated cuprates [9]) theoretically interpreting the experimental observation of ZRS at low doping, and predicting other ZRS related effects at doping levels not experimentally attained so far.

We point out that this is the first instance of a first-principles density-functional-theory-based band approach predicting or describing the formation of ZRS, which are usually studied within Hubbard-like models [1] with simplified electronic structure. While often (perhaps questionably) dismissed as inessential in 2D cuprates, a realistic material-specific description is unquestionably necessary in the context of 1D cuprates. By and large, first-principles calculations have long been absent from this arena due to their difficulties in treating strong correlated cuprates [10].

1D cuprates are chain-like aggregations of weakly coupled chains of CuO_2 units. Compared to other 1D systems (e.g. GeCuO_3 or Sr_2CuO_3) CaYCuO has the advantage [4] of being hole-dopable in a wide range. Magnetization and electrical conductivity measurements [4, 5, 6, 7] in the range $x/n=[0,0.4]$ (here x is the hole concentration and n the number of CuO_2 units per chain, and x/n the hole fraction per

Cu) show that CaYCuO is an antiferromagnetic (AF) wide-gap Mott insulator at $x/n=0$ and a Curie-Weiss AF insulator with one-dimensional hopping-conductivity at $x/n<0.3$. At $x/n\sim 0.3$ the AF susceptibility spreads out in a broad maximum, the signature of a magnetic chain populated by a high density of spinless sites (ZRS). The conductivity is thermally activated with a gap of 0.08 eV. Thus, perhaps surprisingly, the system is effectively insulating through all the experimental doping range. No data are reported for concentrations higher than $x/n=0.4$. Here we deliver a microscopic description of CaYCuO up to full doping $x/n=1$, explaining the mechanism of the observed phase transitions, and uncovering further, not yet experimentally accessible doping effects.

Structure - CaYCuO (Fig.1) is made of ferromagnetic (FM) CuO_2 chains (Cu-Cu separation 3.4 Å, Cu-O-Cu angle $\simeq 90^\circ$) running along y and parallel to the (x, z) plane [4, 5, 6]. Intercalated Ca/Y chains, parallel to the CuO_2 ones, act as electron reservoir for the CuO_2 units. In the synthesized compound $\text{Ca}_{2+x}\text{Y}_{2-x}\text{Cu}_5\text{O}_{10}$ the ratio of Ca/Y and CuO_2 chain steps is 4/5, with $n=5$. Contiguous chains are weakly coupled antiferromagnetically (AF) along z , with $T_N\sim 28$ K at $x=0$ (16 K at $x/n=0.2$). Coupling along x is negligible. To gain computational flexibility, we treat n as a free parameter (as electronic properties depend on x/n but not on n) and perform calculation for $n=2,3,4$. We use a plane-wave ultrasoft-pseudopotential method, with 30 Ryd cut-off and $10\times 10\times 10$ k-point grids; for density of states (DOS) calculations, the linear-tetrahedron interpolation is used on the same mesh. Full details will appear in a forthcoming paper.

Undoped CaYCuO - The calculated orbital-resolved DOS in Fig.2 show that undoped ($x=0$) CaYCuO is a Mott insulator with a gap of 3.44 eV and Cu magnetic moment of $0.71 \mu_B$ (near-gap bands are shown and discussed in Fig.4 below). No experimental gap value is available, but previous studies for low-dimensional cuprates [9] suggest our prediction to be sensible. We obtain the observed magnetic ordering as energetically stable, with FM intra-chain exchange-interaction $J_y=8.5$ meV and AF inter-chain $J_z=-0.2$ meV (~ 7 meV and ~ 1 meV experimentally).

Our calculation attests that CaYCuO is a proper Mott-Hubbard insulator, i.e. valence band top (VBT) and conduc-

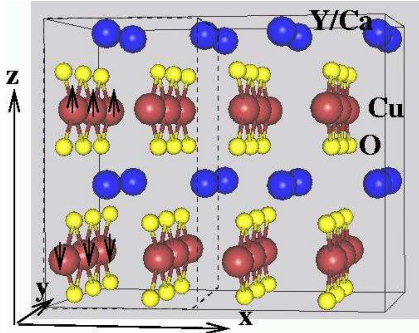


FIG. 1: Structure of CaYCuO. FM y -parallel Cu chains couple antiferromagnetically in the z direction. Dashed lines delimit the orthorhombic lattice with lattice units is 1

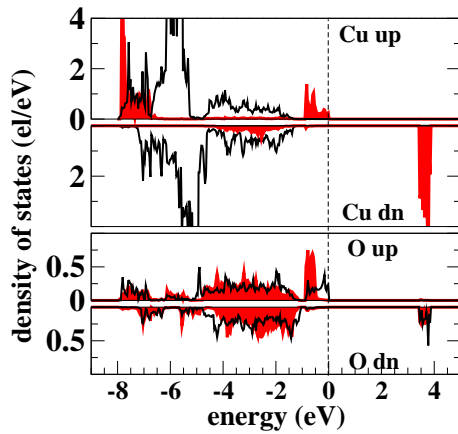


FIG. 2: (Color online) Orbital-resolved DOS for undoped CaYCuO. For Cu the contribution of spin-polarized d_{yz} orbital is represented by the (red) filled line, while the (black) solid line sums up the other four d orbitals. For O, solid and filled lines represent p_y and p_z states, respectively. No Y or Ca DOS appear in this energy range.

tion band bottom have the same orbital character. All Cu are in the $2+$ (d^9) state with the highest d_{yz} orbital spin-polarized. The flat DOS peak located at VBT and separated from the lower-lying valence manifold is due to Cu d_{yz} -O (p_y , p_z) hybrid bands originating from intra-chain FM coupling. The magnetization is about 70% Cu d_{yz} and 15% from each adjacent oxygen. The gap opens between up- and down-polarized channels of these p - d hybridized bands. It is worth noting that a standard density-functional calculation predicts a non-magnetic metal.

Doped CaYCuO: Fig.3 summarizes the calculated properties vs. doping. Fig.4 reports the corresponding band structures. We find three markedly different regions corresponding to hole concentration ranges $0 < x/n < 1/4$, $1/3 < x/n < 1/2$, and $1/2 < x/n < 1$. The $x/n=1$ case stands out separately, as discussed below.

a) Underdoped region – At low concentration ($0 < x/n < 1/4$)

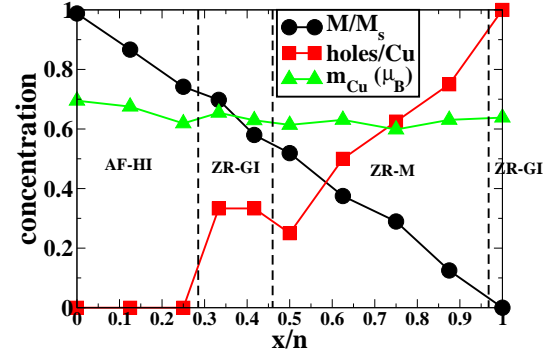


FIG. 3: (Color online) Calculated properties as a function of doping. Black circles are relative FM chain magnetization per CuO_2 unit, green triangles are Cu magnetic moment, red squares are the averaged number of ZRS per CuO_2 unit. Going from $x=0$ to $x=1$ system changes from AF Mott insulator ($x=0$) to AF hopping insulator (HI), ZR gap insulator (GI), ZR metal (M), ZR Mott insulator (at $x=1$).

injected holes empty progressively the p - d hybridized VBT peak, without major changes in the band shape: the injected charge disperses along the chain, and no ZRS forms. The chain magnetization decreases almost linearly with x , the AF alignment remaining unaffected. As for conduction, Fig.4 shows that at $x/n=1/4$ (one hole every four CuO_2 units) only the very flat (d_{yz} - p_y , p_z) spin-majority bands are cut by E_F , and then only in the k_x , k_z -parallel segments M-R and M'-M, orthogonal to the chains. Therefore the system is a low-mobility hopping-conductive insulator. This region is characterized (Fig.3) by zero ZRS concentration (red squares), a smooth linear decrease of relative chain magnetization (black circles), and a weak decrease of Cu magnetic moment (green triangles).

b) ZRS gap insulating region – As doping nears the threshold $x/n=1/3$, ZRS populate the system: spin-polarized holes localized on the oxygens are coupled with the spin-antialigned holes on the adjacent Cu, so the total magnetic moment of the corresponding CuO_2 unit is $S=0$. This occurs because hole-hole Coulomb repulsion exceeds the Cu-O charge transfer energy, favoring hole localization. This doping regime exhibits a gapped behavior, with transport properties dominated by optical absorption conductivity. Again we note that a standard local-density calculation would not obtain hole localization, hence no ZRS.

Fig.5 shows DOS and magnetization isosurfaces for $x/n=1/3$. At this concentration the holes are fully localized, and form one ZRS each three CuO_2 steps. Two band features signal the presence of ZRS. The first is the flat states of the doping-injected holes, strictly localized on oxygens and with marked p_z character, at ~ 0.4 eV above the VBT. The second signature is the ~ 1 eV downshift (from the undoped value) of part of the Cu d_{yz} spin-minority bands. An antialigned pair of spin-majority p_z and spin-minority d_{yz} adjacent holes couple to form one ZRS, whereas the d_{yz} spin-minority Cu states not coupled to any localized hole (i.e. not engaged in a ZRS) remain in the undoped-like position ~ 3.5 eV above VBT.

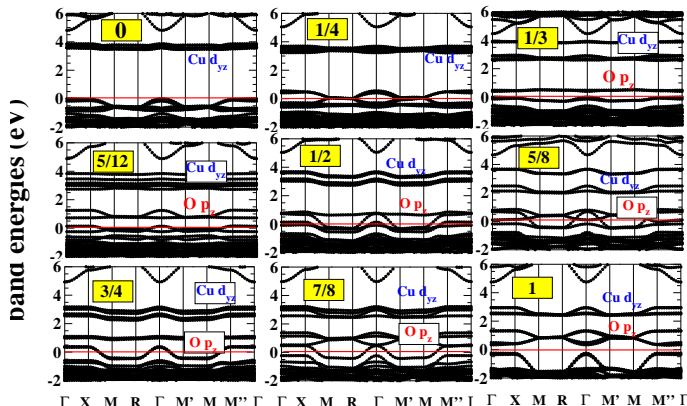


FIG. 4: Band energies at various dopings: system is hopping-conductive up to $x/n=1/4$, gap-insulating until $x/n=1/2$, metallic above $x/n=1/2$, gap-insulating at both end-points $x/n=0$ and $x/n=1$.

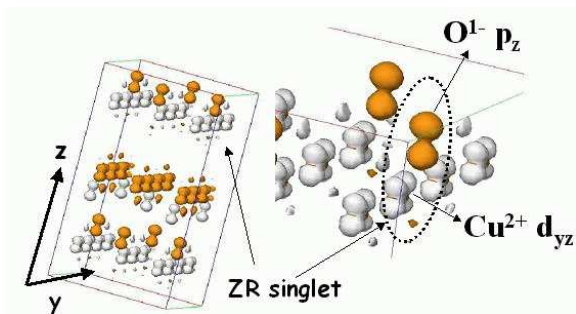
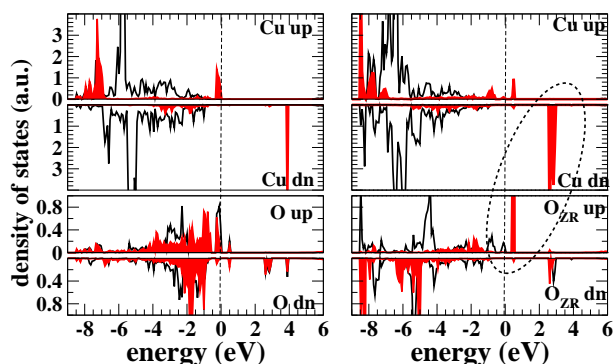


FIG. 5: (Color online) Upper panel: orbital resolved DOS of CaY-CuO at $x/n=1/3$ (non-ZRS, left; ZRS, right). Holes localize on O p_z states ~ 0.4 eV above VBT, and couple to adjacent Cu d_{yz} states (at ~ 2.5 eV). The p_z and d_{yz} orbitals (enclosed by ovals) are anti-aligned, i.e. the two-particle system is a singlet (ZRS). Lower panel: hole density isosurfaces ($h=0.027$ bohr $^{-3}$) for states within 4 eV above VBT. White and gray (yellow) surfaces are up and down polarized holes. In blow-up, the ZRS-forming anti-aligned p_z and d_{yz} orbitals are highlighted by a dashed circle.

The ZRS is clearly visible in the spin-polarized hole charge isosurfaces of Fig.5. Furthermore, ZRS formation shows up in the calculated magnetic moments in Table I. Non-ZRS Cu and O atoms keep their undoped-state magnetic moment. In the units hosting the localized holes, Cu and O's compensate each other quite exactly, forming a ZRS.

TABLE I: Orbital contributions to magnetic moments. "Cu, O" refer to non-ZRS units, "Cu*, O*" to ZRS units. In the latter, the opposite magnetizations on d_{yz} and p_z states dominate: the corresponding CuO $_2$ unit is demagnetized ($S \approx 0$).

$M(\mu_B)$	d_{yz}	p_x	p_y	p_z	Total
Cu	0.65				
O		0.0	0.1	0.1	
Non-ZRS					0.67
Cu*	0.68				
O*		-0.02	0.05	-0.68	
ZRS					0.03

As discussed e.g. in [4, 5, 6, 7], the low doping-to-ZRS phase transition is associated to a change from AF to some disordered paramagnetic (cluster spin-glass or spin-liquid) mixture of ZRS and small residual FM chain segments. Indeed, consider in Fig.3 the difference between CuO $_2$ (black circles) and Cu (green triangles) contributions to the average magnetization. The former drops linearly through the whole doping range, since holes deplete spin-majority states (either O p or Cu d) at any x/n . Cu magnetization, instead, decreases linearly only in the low-doped region, but as soon as ZRS appear, it remains roughly constant up to $x/n=1$. This means that as x increases, ZRS formation demagnetizes more and more CuO $_2$ units, progressively destroying the chain FM ordering, while leaving Cu magnetic moments at about their undoped values. (SQUID susceptibility data [7] also suggest ordered ZRS patterns, but calculations for these structures exceed our present computing capabilities.)

c) High-doping ZRS-rich metallic region - As x increases, the number of ZRS increases as long as the hole concentration is large enough to allow the "condensation" of more holes on the oxygens. However, as the average hole-hole distance is reduced, the charge associated to each ZRS spreads out: at $x/n=1/2$ (i.e. one ZRS per two CuO $_2$ unit), injected holes no longer localize on a single oxygen, but spill out on adjacent CuO $_2$ units. The corresponding states span a ~ 1 -eV energy range, much larger than the optical gap of the ZR-GI regime and also larger than the undoped VBT DOS peak. As a consequence, the high-doped ($x/n > 1/2$) ZRS-rich region is weakly metallic, although large resistivity should still be expected due to the small band dispersion. Since metallic ZRS capture a larger hole charge fraction than insulating ZRS present at $x/n=1/3$, at $x/n=1/2$ some of the chains remain ZRS-free, thus causing the ZRS concentration drop visibly in Fig.3 in correspondence of the metal-insulating transition.

According to the hole isosurface plots in Fig.6, in this regime the systems has no recognizable magnetic order, and can be seen as a disordered mixture of impure ZRS (i.e. with S not exactly zero: due to metallicity O and Cu polarized states do not compensate exactly) and CuO $_2$ units with varying magnetization. (These features will be illustrated below in an overview of the evolution of magnetic ordering and band energies vs x/n .)

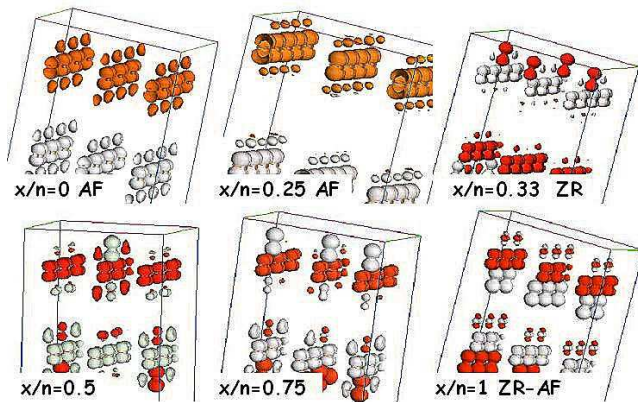


FIG. 6: Hole density isosurfaces (same as Fig.5) at various dopings: up to $x/n=1/4$ the original AF ordering still rules; at $x/n=1/3$ ZRS form, and one each 3 CuO_2 units form a singlet; intra-chain FM ordering is lost, and system is cluster spin glass or paramagnetic. Above $x/n=1/2$ more than 50% of CuO_2 has $S=0$, i.e. system becomes more and more non-magnetic.

d) ZRS-saturated diamagnet - The above picture holds for increasing doping, until at $x/n=1$ (i.e. one hole for each CuO_2 unit) our calculations predict an exotic ZRS-saturated insulating regime, where each CuO_2 hosts one ZRS. The system is now a collection of singlet states, hence a non-magnetic (in fact diamagnetic) insulator, despite Cu magnetic moments still close to their undoped values. It would be exciting to push the experimental doping limit up to $x/n=1$ and verify the validity of this prediction.

Overview- In Fig.6 several frames of hole density isosurfaces are shown as a function of doping. This juxtaposition highlights the evolution from low-doping intra-chain FM ordering to ZRS ordering: for $x/n < 1/3$ all O and Cu holes are parallel-oriented (thus CuO_2 magnetization is larger than the Cu magnetic moment) and hole isosurfaces can hardly be distinguished from their undoped counterpart at $x/n=0$. With ZRS formation, holes collapse onto O-centered p_z -shaped charges, antiparallel (different color in the Figure) to the d_{yz} -shaped Cu holes. On the other hand, the small hole density residing on non-ZRS oxygens remains spin-parallel (equally colored) to Cu holes. The change from ZRS insulating to metallic regime ($x/n \sim 1/2$) shows up in the irregular hole-charge distributions on the oxygens: now even non-ZRS oxygens can give intra-chain AF contributions to the total chain magnetization (because of ZRS broadening to the nearby CuO_2 units).

The calculated band structure vs x/n in Fig. 4 con-

firms again the two regime changes mentioned earlier. The transition from low-doping hopping-conductive to ZRS gap-insulating at $x/n=1/3$ is characterized by the flat oxygen bands at ~ 0.4 eV above the VBT. Thus, in the region $1/3 < x/n < 1/2$ we expect transport properties to be dominated by optical absorption through this energy gap. Above $x/n=1/2$ the optical gap closes due to ZRS spreading out over the chains. At $x/n=1$ the spectrum is gapped once again: one spin-polarized hole per CuO_2 is exactly what is needed to empty out the flat p-d bands present at the VBT of the undoped system (see Fig.2).

In conclusion, we described ZRS formation and properties in a doped 1D cuprate using a first-principles band theory. We interpreted in detail the observed simultaneous change of magnetic and transport properties of CaYCuO upon doping, and extended the analysis to dopings not (yet) reachable experimentally. The fact that a first-principles band theory proved able to describe ZRS formation in a doped Mott insulator for the first time is an instrumental step for a realistic description of a wide class of low-dimensional doped cuprates.

Acknowledgments Work supported in part by MiUR (Italian Ministry of University) through projects PON-Cybersar and PRIN 2005, and by Fondazione Banco di Sardegna (Project Correlated oxides).

-
- [1] F. C. Zhang and T. M. Rice, Phys. Rev. B **37**, 3759 (1988); H. Eskes and G. A. Sawatzky, Phys. Rev. Lett. **61**, 1415 (1988).
 - [2] N. B. Brookes, G. Ghiringhelli, O. Tjernberg, L. H. Tjeng, T. Mizokawa, T. W. Li, and A. A. Menovsky, Phys. Rev. Lett. **87**, 237003 (2001).
 - [3] P. W. Anderson, P. A. Lee, M. Randeria, T. M. Rice, N. Trivedi, and F. C. Zhang, J. Phys.: Condensed Matter **24**, Topical Review R755 (2004).
 - [4] A. Hayashi, B. Batlogg, and R. J. Cava, Phys. Rev. B **58**, 2678 (1998), and references therein.
 - [5] H. F. Fong, B. Keimer, J. W. Lynn, A. Hayashi, and R. J. Cava, Phys. Rev. B **59**, 6873 (1999).
 - [6] M. Matsuda, H. Yamaguchi, T. Ito, C. H. Lee, K. Oka, Y. Mizuno, T. Tohyama, S. Maekawa, and K. Kakurai, Phys. Rev. B **63**, 180403 (2001).
 - [7] M. D. Chabot and J.T. Markert, Phys. Rev. Lett. **86**, 163 (2000). Phys. Rev. B **41**, 7892 (1990).
 - [8] A. Filippetti and N. A. Hill, Phys. Rev. B **67**, 125109 (2003).
 - [9] A. Filippetti and V. Fiorentini, Phys. Rev. Lett. **95**, 086405 (2005); Phys. Rev. Lett. **98**, 196403 (2007); J. Magn. Magnetic Mat. **310**, 1648 (2007).
 - [10] W. E. Pickett, Rev. Mod. Phys. **61**, 433 (1989).